Liquid Crystals
Publication details, including instructions for authors and subscription information:
http://www.informaworld.com/smpp/title~content=t713926090

The mountain defect. A new kind of planar defect in surface stabilized smectic C liquid crystals

Zhiming Zhuang[a]; Aaron G. Rappaport[b]; Noel A. Clark[b]
[a] Department of Physics, University of California, Santa Barbara, California, U.S.A. [b] Department of Physics, Condensed Matter Laboratory and Center for Optoelectronic Computing Systems, University of Colorado, Boulder, Colorado, U.S.A.

To cite this Article Zhuang, Zhiming , Rappaport, Aaron G. and Clark, Noel A.(1993) 'The mountain defect. A new kind of planar defect in surface stabilized smectic C liquid crystals', Liquid Crystals, 15: 3, 417 — 427
To link to this Article: DOI: 10.1080/02678299308029142
URL: http://dx.doi.org/10.1080/02678299308029142

LIQUID CRYSTALS, 1993, VOL. 15, NO. 3, 417–427

The mountain defect

A new kind of planar defect in surface stabilized smectic C liquid crystals

by ZHIMING ZHUANG†, AARON G. RAPPAPORT‡
and NOEL A. CLARK‡

† Department of Physics, University of California, Santa Barbara, California 93106-9530, U.S.A.
‡ Department of Physics, Condensed Matter Laboratory and Center for Optoelectronic Computing Systems, University of Colorado, Boulder, Colorado 80309-0390, U.S.A.

(*Received 14 December 1992; accepted 16 February 1993*)

A new kind of planar chevron defect, which we call the 'mountain defect' due to its mountain-shaped appearance under the microscope, is observed in chevron surface stabilized smectic C liquid crystal cells for both chiral (ferroelectric) and achiral materials. Polarized optical microscopy investigations reveal that this kind of defect, which can either appear spontaneously and grow slowly over days, weeks and months or can be induced by applying an electric field or mechanical distortion, mediates change in the chevron interface position, separating chevron domains of differing chevron interface position. The full three dimensional layer structure of this defect and its relation with other commonly seen line defects in such cells, like zig-zag walls and field lines, will be presented. The formation of this kind of defect indicates that chevron structure is not necessarily a stable structure in these cells.

1. Introduction

The layer structure and the unique geometry of surface stabilized smectic C (S_C) liquid crystals (SSSCLC) [1] cells make them susceptible to layering defects. These defects, appearing as lines through polarized light microscopy, mar the homogeneity of the LC molecular alignment inside the cells and reduce the contrast of their electrooptic responses. Therefore understanding the origin and structure of these defects has been an intense area of research, particularly for surface stabilized ferroelectric liquid crystals (SSFLCs). Previously Rieker *et al.* [2–4] using high resolution X-ray scattering, revealed the three dimensional layer structure of one of the most commonly seen defects in SSFLC cells, the zig-zag defect, and identified the chevron structure as the dominant local layer structure (LLS). They pointed out that the zig-zag defect is the layer structure which mediates the change in chevron direction without influencing the layer position at the FLC–solid interfaces [3, 4]. Recently Xue [5] and Willis *et al.* [6] demonstrated the origin and layer structure of another commonly observed layer defect, the field line [7, 8] (which, because of its appearance, is also known as 'boat wake', or 'rooftop'), generated by applying a reasonably high voltage across a chevron SSFLC cell. In this paper we report a new kind of S_C layering defect in surface stabilized

* Author for correspondence.

0267–8292/93 $10·00

geometry, which we call the mountain defect because of its mountain-shaped appearance under the microscope. This defect has been found in both chiral (ferroelectric) and achiral SSSCLC cells and, as we will show, requires a shift in the layer position at the FLC–solid interface.

When Clark and Lagerwall first proposed the SSFLC concept [1], they supposed that the S_C^* layers were oriented nearly perpendicular to the glass substrates (the bookshelf geometry). But this idealized geometry cannot fully explain many observed features of SSFLC cell structure like the existence of the zig-zag defects [9, 10] and the selective pretilt of the spontaneous polarization at the substrates even with planar surface treatments [11] and electrooptic behaviour such as multistate switching [9]. These experimental observations led to X-ray scattering investigations of SSFLC cells and the dicovery of the chevron LLS. The confirmation of the chevron layer model opens the possibility of many other layering defects in chevron SSFLCs, and the mountain defect is one of them. In this paper we present the structure of mountain defects, which is understood quite well, and discuss their origin, which is understood rather poorly.

2. Experimental observations: chiral (SSFLC) cells

We have found mountain defects with a variety of SSFLC cell preparations. For the work reported here, the mountain defects were observed in chevron SSFLC cells with the usual planar surface alignment treatment. Cells were aligned using parallel rubbed nylon films coated on both bounding glass plates. Figure 1 (*a*) shows the general appearance, through a polarized optical microscope, of the mountain defect lines (indicated by the black arrow) in a 3 μm thick SSFLC cell of the material Chisso 1014, phase sequence:

$$X \xleftrightarrow{-21^\circ C} S_C^* \xleftrightarrow{54^\circ C} S_A \xleftrightarrow{69^\circ C} N^* \xleftrightarrow{81^\circ C} I.$$

The pink background area appeared immediately after the cell was cooled into the S_C^* phase. For this particular cell, after being left in the S_C^* phase for several hours, a yellow coloured region with mountain shaped boundaries, which nucleated at the S_A to S_C transition, grew from the edges into the centre of the cell. Mechanical distortions to the cell, such as adjusting the screws in the sample holder at the time when the S_A to S_C transition occurs, could also generate mountain defects.

The spatial relationship between the mountain defects and zig-zag walls is demonstrated in figure 1 (*b*). We can see clearly in this photograph that the zig-zag walls (indicated by the white arrow) can run across the mountain defects, indicating that mountain defect is a different kind of defect than the zig-zag wall and the chevron layer structure is maintained on both sides of the mountain defect line. It is worth noting, however, that there is little change in both zig-zag wall direction and width when it goes across the mountain defect line, which strongly suggests that the layer tilt angle is the same across the mountain defect since both the direction and the width of the zig-zag line depend on the layer tilt angle [12]. This is important evidence which we shall use in developing our three dimensional model for this defect.

Evidence that the chevron interface position shifts upon crossing the mountain defect line can be obtained from the response of the cell to applied fields, as is shown in figure 2. Figures 2 (*a*) and (*b*) depict the switching process at the chevron interface, characterized by the boat-shaped interfacial orientational domains [3, 4, 11] outside the region surrounded by the mountain defect. The applied voltages are

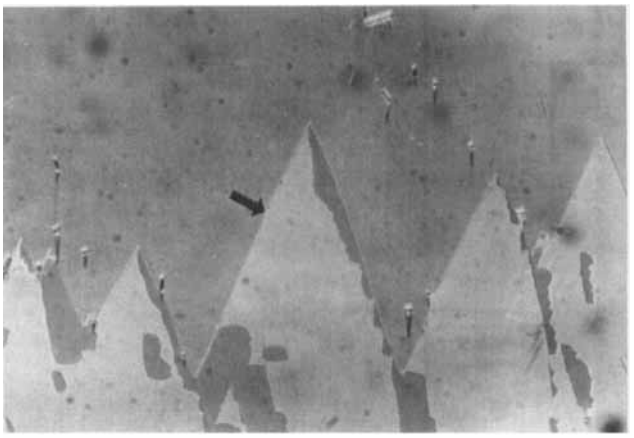

(*a*)

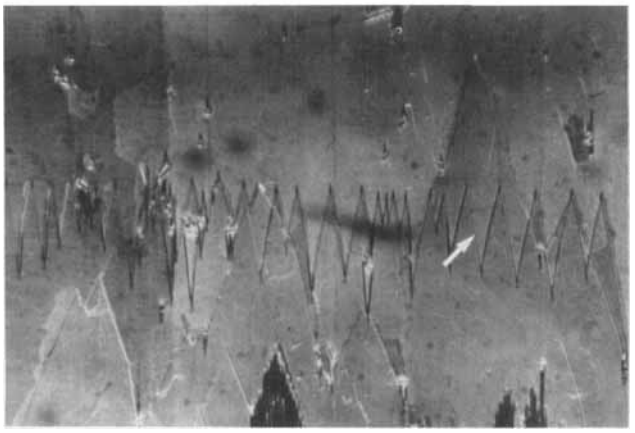

(*b*)

Figure 1. Mountain defect lines (black arrow) in a 2 to 3 μm thick Chisso 1014 cell. The defect line forms the boundary between two areas having the chevron interface at different levels between the ITO coated bounding plates. The white arrow shows a zig-zag line where the chevron layer bend changes sign.

$-0{\cdot}26$ V and $+0{\cdot}06$ V for photos (*a*) and (*b*), respectively. It is clear that in both directions of the switching processes, the area outside the mountain defect switches simultaneously on both sides of the zig-zag wall, a characteristic behaviour for the symmetric chevron structure (chevron interface located in the middle of the cell) in which both bistable states are energetically degenerate [4, 13]. The next four photographs in figure 2 show the chevron interface transitions inside the region surrounded by the mountain defect. The applied voltages are $-0{\cdot}45$ V, $-0{\cdot}25$ V, $+0{\cdot}15$ V and $+0{\cdot}28$ V for photos (*c*), (*d*), (*e*) and (*f*), respectively. First we notice that only the region on one side of the zig-zag wall switches at a time. Second, for each region on one side of the zig-zag wall the switching voltages have the same sign (either plus or minus) for both directions of switching. All these phenomena indicate one of the bistable states is energetically more favourable than the other, a typical consequence of an asymmetric chevron structure (the chevron interface not located in the middle of the cell) because the state that has the twisted part of the director profile in the thick portion of the chevron has a lower elastic free energy [13].

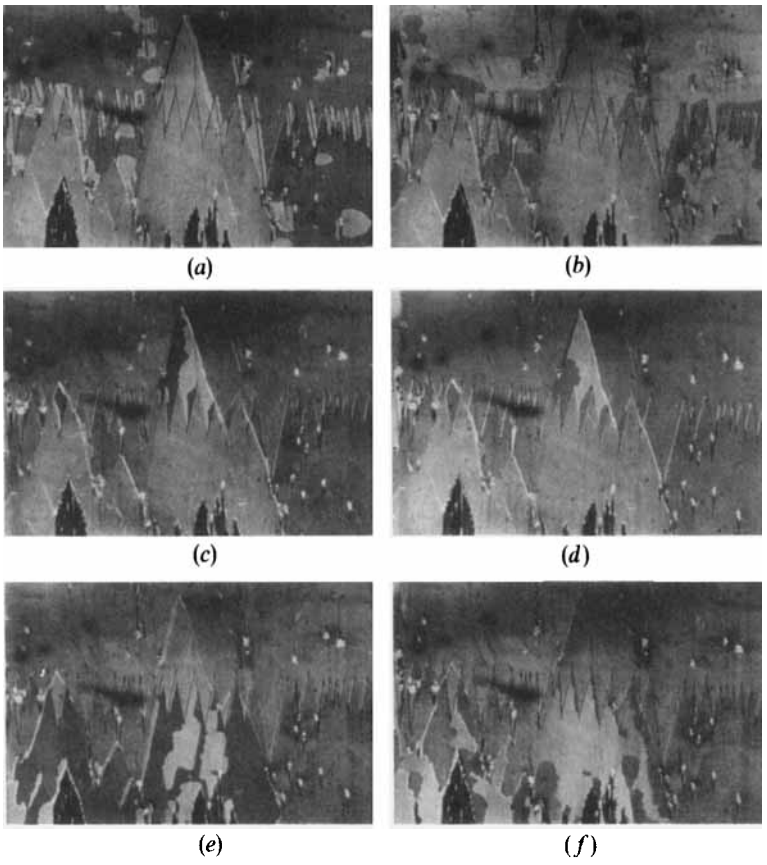

Figure 2. This sequence shows that the switching thresholds for polarization reversal at the chevron interface changes as the mountain defect line is crossed. This is in accord with expectations for half-splayed states [13].

When we applied a sufficiently high field across the cell, field lines [5–7] were generated. The relationship between the field lines and mountain defects is demonstrated in the two photographs in figure 3. Field lines can be nucleated at the mountain defect lines. This fact indicates that smectic layers have a smaller vertical layer tilt angle within the interior of the mountain defect lines than they have outside it. The angle the mountain defect lines make with respect to the layer normal is about the same as that of the field lines. The local layer structures should be similar between these two kinds of line defects.

3. Experimental observation: achiral cells

Mountain defects were observed in chevron achiral SSSCLC cells as well, which confirms that they are a layering defect associated with the chevron S_C layer structure but not requiring chirality. Figure 4 shows the generation of the mountain defects in an achiral cell. The liquid crystal material used here is $\bar{8}S5$, which is a monotropic S_C material with the phase sequence

$$X \xleftarrow{19{\cdot}4^\circ C} ? \xleftarrow{31{\cdot}3^\circ C} S_C \xleftarrow{56{\cdot}3^\circ C} S_A \xleftrightarrow{63{\cdot}5^\circ C} N \xleftarrow{86{\cdot}5^\circ C} I.$$

$$\xrightarrow[58{\cdot}6^\circ C]{}$$

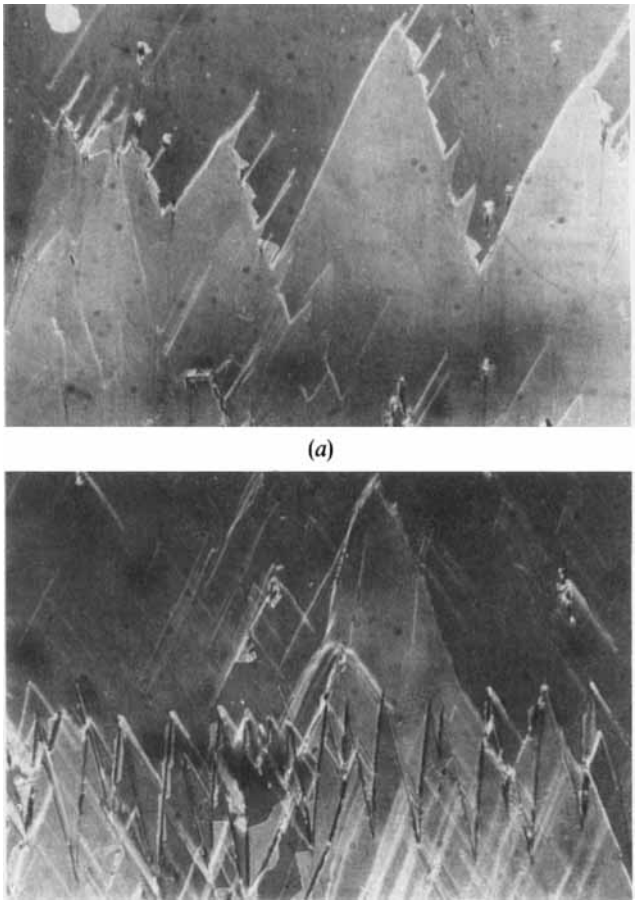

(*a*)

(*b*)

Figure 3. Sufficiently large electric fields generate 'roof-top' field lines [5–7], which tend to nucleate on the mountain defect lines. The mountain defects are not otherwise affected by applied fields in chiral smectic C cells.

and the cell thickness is about 4 μm with parallel rubbed polyimide films coated on both inner surfaces of the cell as alignment layers.

Figure 4(*a*) gives the general texture of this achiral SSSCLC cell seen through a polarized microscope when the cell was first cooled down into the S_C phase. Parts of the zig-zag loops are shown clearly in the picture. There were a variety of surface stabilized director states separated by sharp domain lines with zero field applied, shown here as the dark green and the light green states, which corresponded to the two states with director uniformly aligned along either intersection direction of the S_C tilt cone and the glass plates, and the red and yellow states, which were twisted states in opposite sense which could be generated via field application with a well-defined threshold that depended on the chevron interface position. The lack of polar surface interaction [9] due to the achiral nature of the LC material made these states possible. They will be discussed in detail elsewhere [14].

In the $\bar{8}S5$ cell mountain defects could be generated by the application of an electric field. This is in contrast to the chiral cells where the application of a sufficient field

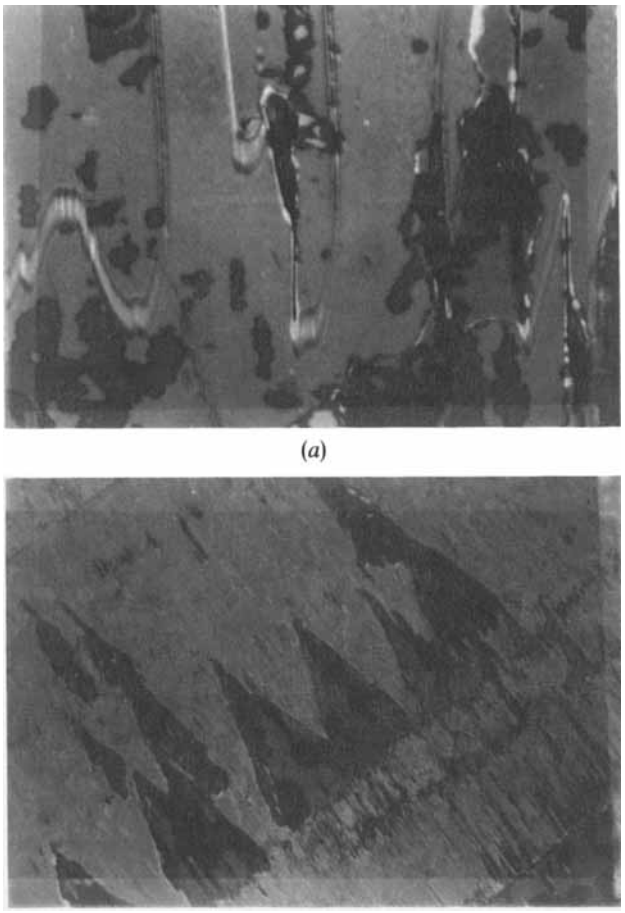

(*a*)

(*b*)

Figure 4. Zig-zag defects and mountain defects in a 4 μm thick cell filled with an achiral smectic C material (8S5). These mountain defects were generated by application of an electric field.

generates field lines but not the mountain defects. When a high amplitude AC field (75 V_{p-p}) was applied to the cell at $T = 0°C$ for several minutes, the mountain defects started to appear, as shown in figure 4 (*b*). A DC applied field could also result in mountain defect generation. The major coupling between the LC and external field here was the dielectric effect due to the positive dielectric anisotropy of $\bar{8}S5$, rather than ferroelectric effects as in the chiral case. The mountain defect formation process was irreversible, that is, once formed they remained after the field was removed. In order to visualize the mountain defects a small voltage was applied and the cell was oriented to maximize the contrast between the mountain area and the rest of the cell. Studies at different temperatures showed that the mountain defects took much less time to form near the S_A to S_C phase transition. Evidence that the chevron interface changed its position across the mountain defect line was again provided by the differences in the field induced director switching processes in the two regions separated by the defect lines. For the defects of figure 4 (*b*), within the new region generated by the growth of the mountain defect line, there were fewer director states observed during the switching than in the original region, indicating the absence of the chevron interfaces in the new

region [14]. This is the extreme limit of the displacement of the chevron interface in which it is eliminated to form a tilted layer structure ($r_1 = 1$ in figure 6(*b*)) in the new region.

4. Local layer structure of the mountain defect

We now summarize the evidence of the layer structure of the mountain defects gathered through experimental observations. The following equations govern the geometry of the zig-zag walls [4, 12]

$$\frac{\cos(\alpha-\gamma)}{\cos(\gamma)} = \cos\delta, \tag{1}$$

and

$$w = t\frac{\cos(\gamma)\sin(\delta)}{\sin(\alpha)}, \tag{2}$$

where γ is the angle the zig-zag lines make with the projection of the smectic layer normal on the substrate plane (z axis), α is the angle between the projections of the normal of the layers in the interior of the defect line and the normal of undistorted layers on the substrate plane (z axis), δ is the layer tilt angle, t is the cell thickness, and w is the width of the zig-zag line. We know from figure 1(*b*) that zig-zag walls can run across the mountain defect line without noticeable change in both direction (γ) and width (w). It is easy to determine from the above equations that the angle δ also cannot change across the mountain defect line. The switching process shown in figure 2 tells us that the mountain defect mediates a change in chevron interface position, and in this particular cell it separates domains with symmetric and asymmetric chevron structure. The fact that the mountain defect lines are nucleation sites for the field lines (figure 3) indicates that some part of the layers in the interior of a mountain defect line have a smaller tilt angle than the layers outside the defect line.

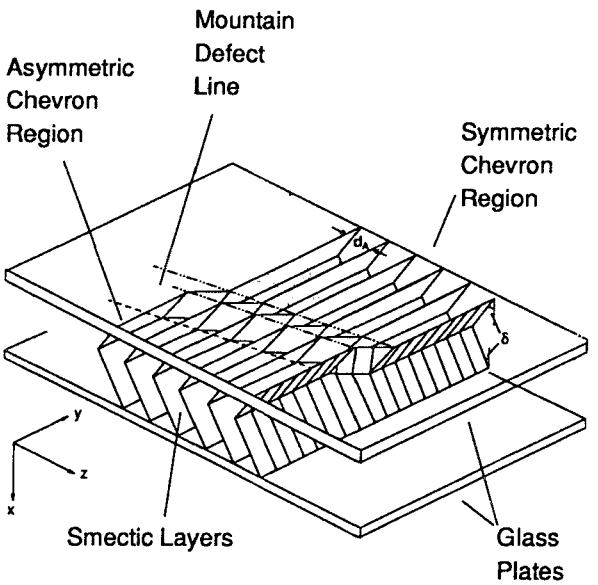

Figure 5. Schematic diagram of the layer structure which we propose for the mountain defect lines. These lines form the boundary between regions of differing chevron interface position along x.

From the experimental evidence and the principle that any layer reorientation and reconnection at the substrate surface must be minimized to reduce the energy cost, we have developed the three dimensional structure shown in figure 5. The major features of this model are as follows: the layer structure on one side of the chevron interface is undistorted across the mountain defect line (the fact that the layer tilt angle is the same on both sides of the defect line enabled us to make this assumption, which reduces the layer reorientation and reconnection within the defect line to only one of the substrate surfaces); the smectic layer spacing is chosen to be d_C everywhere to reduce the bulk distortion free energy; the layering pitch (distance per layer along z) outside the defect at both substrate surfaces is fixed at d_A as is commonly assumed in chevron SSFLC cells. The pitch at one of the substrates within the interior of the mountain defect line is $d < d_A$ so that the reoriented segment joining the layer across the defect line can have a smaller layer tilt angle; for simplicity, there are no dislocations inside the defect, the layers are continuously connected. Although the existence of layer dislocations is essential in the nucleation and growth of the mountain defect, as discussed later, their effects on local geometrical relations inside the defect are relatively small.

Figure 6 gives three different views of our proposed structure of a mountain defect line. Several geometrical relations can be obtained from this figure, which give the constraints on the structural parameters of the cell, the smectic layers, and the defect.

(i) Consider the two adjacent triangles containing the length d_A and d in figure 6(*a*). The side they share can be used to derive the relationship between d_A and d

$$\frac{d}{\cos(\chi+\gamma)}=\frac{d_A}{\cos(\gamma)}. \tag{3}$$

(ii) The assumption that the layer spacing is d_C everywhere provides us with three equations

$$\frac{d_C}{d_A}=\cos(\delta), \tag{4}$$

$$\frac{d_C}{d}=\cos(\delta') \tag{5}$$

and

$$l=\frac{d_C}{\cos(\chi)\cos(\delta')}. \tag{6}$$

(iii) To match the layer spacing along the dotted lines in figure 6(*c*) we get the following equations for angles α and β

$$\frac{d_C}{\cos(\delta-\beta)}=\frac{l\cos(\delta'')}{\cos(\beta+\delta'')}, \tag{7}$$

$$\frac{d_C}{\cos(\alpha-\delta)}=\frac{l\cos(\delta'')}{\cos(\alpha+\delta'')}, \tag{8}$$

and

$$L=(1-r_2)t\cot(\alpha)+(r_1-r_2)t\cot(\beta). \tag{9}$$

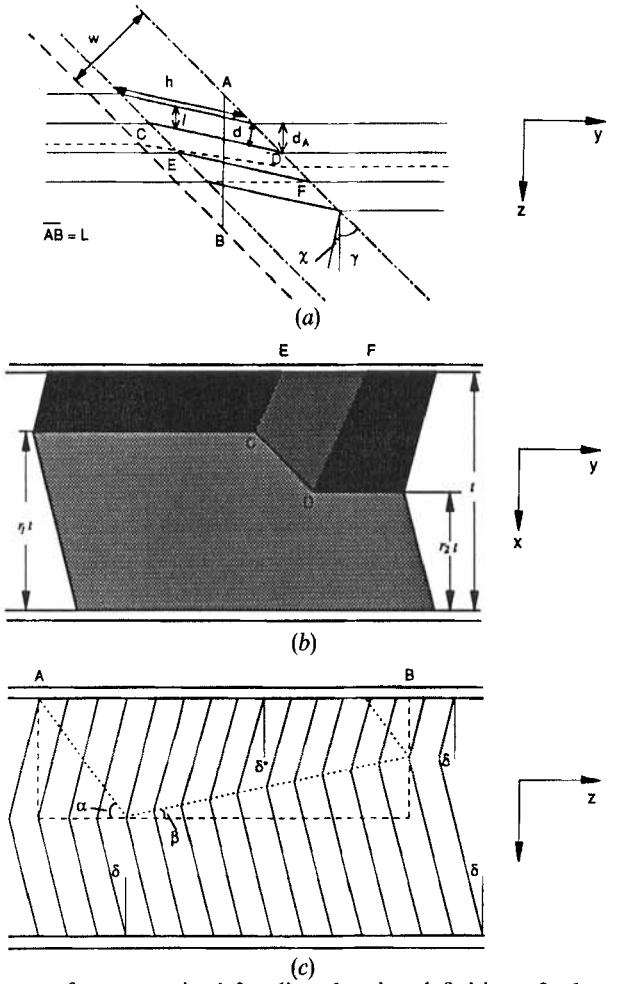

Figure 6. Geometry of a mountain defect line showing definition of relevant distances and angles.

(iv) Finally, it is easy to find the relationship between L and w, the width of the mountain defect lines using figure 6(*a*)

$$w = L\sin(\gamma). \tag{10}$$

The angles α and β can be determined using the equations (6), (7) and (8) along with the relation $\tan(\delta') = \tan(\delta'')\cos(\chi)$

$$\cot(\alpha) = \frac{\sin(\delta) - \sin(\delta')}{\cos(\chi)\cos(\delta') - \cos(\delta)}, \tag{11}$$

$$\cot(\beta) = \frac{\sin(\delta) + \sin(\delta')}{\cos(\chi)\cos(\delta') - \cos(\delta)}, \tag{12}$$

which with equations (9) and (10) give the width of the mountain defect line

$$w = \frac{t}{\cos(\chi)\cos(\delta') - \cos(\delta)}((1 + r_1 - r_2)\sin(\delta) - (1 - r_1)\sin(\delta')). \tag{13}$$

Also from equations (3) and (4) we have

$$\frac{\cos(\delta)}{\cos(\delta')}=\frac{\cos(\chi+\gamma)}{\cos(\gamma)}, \tag{14}$$

which can be rewritten as

$$\tan\gamma=\frac{\cos(\chi)\cos(\delta')-\cos(\delta)}{\sin(\chi)\cos(\delta')}. \tag{15}$$

Equations (13) and (15) are the two major geometrical relations governing the appearance of the mountain defect. As it is in the case of the zig-zag wall [12] or the field line [5] we have more unknowns than we have equations, so the angle and width of the mountain defects are not uniquely determined by the geometry. There must be some constraints imposed by considerations of the free energy for layer and director distortions. One possible constraint from layer distortion might come from minimizing the angles $\sigma_{\pm}$, the layer segment CDEF in the defect (see figure 6(*b*)) makes with the undistorted part of the layers. These angles are

$$\cos(\sigma_{\pm})=\pm\sin(\delta')\sin(\delta)+\cos(\chi)\cos(\delta')\cos(\delta). \tag{16}$$

We can use equations (13) and (15) to solve the angles δ' and χ and include the results in equation (16). Then minimizing the angles $\sigma_{\pm}$ with respect to γ, we can solve γ and w unambiguously in terms of δ, t, r_1 and r_2, which are geometrical parameters determined by the LC material constant and cell preparation process. Since we do not have the experimental data on r_1 and r_2, we cannot check this model at the moment. An X-ray scattering experiment, which can give us the values of r_1 and r_2, is in preparation at this point.

5. Discussion

Based on these experiments and our knowledge of the chevron layer structure, we conclude the following observations. The shift of the chevron interface in a SSSCLC cell, δ_{rt}, can be produced simply by a relative displacement δ_z of the bounding plates along z, with $\delta_{rt}=\delta_z/2\tan(\delta)$. It is this kind of shift which effectively occurs with the propagation of a mountain defect line, but without the relative displacement of the plates. Thus the shift of the chevron interface in the mountain defects must require some layer reconnections equivalent to the shift of layers parallel to z at one of the plates. Experiments on field induced layer structure changes in SSFLC cells show that the in-chevron structure does not occur readily in layer reconnection. However, recent X-ray experiments [15] indicate the presence of edge dislocations in the S_C chevron structure and a potential mechanism for the elimination of edge dislocations for the layer displacement necessary for the chevron interface shift. In the chiral cells mountain defects form in response to mechanical distortions, and grow slowly as a result of internal stress. The difference in electric field response of the chiral and achiral cells with respect to mountain defects is striking. For the ferroelectric case in which the ferroelectric torques tend to reduce the layer tilt (upright layers) [6], the response is to form field lines at high field. In contrast, in $\bar{8}$S5, where the dielectric torque tends to increase the layer tilt [14], increasing the field always resulted in mountain defects and at sufficiently high field, uniformly tilted layers. This difference in behaviour is not well-understood at this time, although in the dielectric case, field induced director splay at the chevron interface will increase its energy significantly, providing stresses which may tend to expel the chevron interface. In any case the application of a field coupling to the

dielectric anisotropy (for example a high frequency field) of positive dielectric anisotropy material may be a useful way to generate the uniform tilted layer structure.

In conclusion, we have observed a new kind of line defect, the mountain defect, in SSSCLC cells. Polarized optical microscopy investigations reveal that this new line defect mediates a change in chevron interface position with local smectic layer tilt angles that are the same on both sides of the defect line. The formation of this defect indicates that the chevron layer structure is not necessarily a stable (global energy minimizing) structure. A three dimensional local layer structure model is developed for this new line defect. Mechanically and electrically induced defects have been one of the major problems in manufacturing SSFLC devices. The understanding of the mountain defect will give some insights into solving these problems.

This work was supported by U.S. ARO contract DAAL 05-93-G-002, NSF grant CDR 8622236 and Canon, Inc.

References

[1] CLARK, N. A., and LAGERWALL, S. T., 1980, *Appl. Phys. Lett.*, **36,** 899.
[2] RIEKER, T. P., CLARK, N. A., SMITH, G. S., PARMER, D. S., SIROTA, E. B., and SAFINYA, C. R., 1987, *Phys. Rev. Lett.*, **59,** 2658.
[3] CLARK, N. A., and RIEKER, T. P., 1988, *Phys. Rev.* A, **37,** 1053.
[4] CLARK, N. A., RIEKER, T. P., and MACLENNAN, J. E., 1988, *Ferroelectrics*, **85,** 79.
[5] XUE, J.-Z., 1989, Ph.D. Dissertation, University of Colorado.
[6] WILLIS, P. C., CLARK, N. A., XUE, J.-Z., and SAFINYA, C. R., 1992, *Liq. Crystals*, **12,** 891.
[7] DUBAL, H. R., ESCHER, C., and OHLENDORK, D., 1988, *12th International Liquid Crystal Conference*, Freiberg, West Germany.
[8] HARTMANN, W. J. A. M., and LUYCKX-SMOLDERS, A. M. M., 1990, *J. appl. Phys.*, **67,** 1253.
[9] HANDSCHY, M. A., and CLARK, N. A., 1984, *Ferroelectrics*, **59,** 69.
[10] OUCHI, Y., TAKEZOE, H., and FUKUDA, A., 1987, *Jap. J. appl. Phys.*, **26,** L1.
[11] ISHIKAWA, K., UEMURA, T., TAKEZOE, H., and FUKUDA, A., 1985, *Jap. J. appl. Phys.*, **24,** L230.
[12] RIEKER, T. P., and CLARK, N. A., 1992, *Phase Transitions in Liquid Crystals*, edited by S. Martellucci (Plenum), p. 287.
[13] MACLENNAN, J. E., HANDSCHY, M. A., and CLARK, N. A., 1990, *Liq. Crystals*, **7,** 787.
[14] RAPPAPORT, A. G., ZHUANG, Z., and CLARK, N. A., 1992, *14th International Liquid Crystal Conference*, Pisa (in preparation).
[15] WILLIS, P. C., CLARK, N. A., and SAFINYA, C. R., 1992, *Liq. Crystals*, **11,** 581.